



# Cloning, expression, and serological detection of the putative RNA polymerase of Papaya meleira virus Mexican variant in *Escherichia coli*

Wendy Serra<sup>1</sup>, Jeanin A. Arguelles-Quintal<sup>1</sup>, Mildred Carrillo-Pech<sup>2</sup>, Alethia F. Toriz<sup>1</sup>, Enrique Castaño<sup>1</sup>, Ignacio Islas-Flores<sup>1</sup>, Luisa A. Lopez-Ochoa<sup>1\*</sup>. <sup>1</sup>Unidad de Biología Integrativa, Centro de Investigación Científica de Yucatán, A.C., Mérida, Yucatán, México, CP 97205. <sup>2</sup>Unidad de Biotecnología, Centro de Investigación Científica de Yucatán, A.C., Mérida, Yucatán, México, CP 97205.

\*Corresponding Author:  
Luisa López Ochoa  
luisa\_lopez@cicy.mx

Section:  
Periodical Issue

Received:  
01 May, 2024  
Accepted:  
25 April, 2025  
Published:  
30 April, 2025

Citation:  
Serra W, Arguelles-Quintal JA,  
Carrillo-Pech M, Toriz AF,  
Castaño E, et al., 2025.  
Cloning, expression, and  
serological detection of the  
putative RNA polymerase of  
Papaya meleira virus Mexican  
variant in *Escherichia coli*.  
Mexican Journal of  
Phytopathology 43(2): 70.  
<https://doi.org/10.18781/R.MEX.FIT.2405-00>



## ABSTRACT

**Background/Objective.** Papaya meleira disease in Mexico is associated to Papaya meleira virus Mexican variant (PMeV-Mx) and is characterized by the spontaneous exudation of latex in fruits. PMeV-Mx ORF2 encodes a protein with RNA-dependent RNA polymerase (RdRp) motifs, which is essential for viral replication. This study aimed to develop a method for producing and purifying recombinant PMeV-Mx ORF2 encoded protein (pORF2) in *E. coli* and generate specific antibodies for its detection.

**Materials and Methods.** The PMeV-Mx genome was analyzed using UGENE to predict ORFs and identify the putative slippery site. ORF1 and ORF2 were amplified by PCR from cDNA obtained from infected papaya latex, cloned into pGEM-T Easy, and subsequently transferred into pDONR221 and pDEST17 for expression in *E. coli*. Recombinant 6xHis-pORF2 was expressed in *E. coli* BL21 strain, induced with IPTG, and purified under denaturing conditions. The purified protein was used to generate polyclonal antibodies, with immunizations conducted at different time points. Antisera specificity and optimal working dilutions were evaluated by immunodetection assays, using recombinant 6xHis-pORF2 as the target and His-tagged proteins as negative controls. Additionally, papaya plants were inoculated with latex from symptomatic fruits as virus reservoir and PMeV-Mx infection was confirmed by RT-PCR.

**Results.** The recombinant 6xHis-pORF2 protein of PMeV-Mx was expressed in *E. coli* and purified. A ~46.5 kDa band was detected, consistent with its estimated molecular weight. The protein expression increased between 2- and 6-hours post-induction with IPTG. Western blot analysis confirmed the presence of the His-tag and the integrity of the recombinant protein. Purification using Ni-NTA resin resulted in a strong ~46.5 kDa band along with light bands ranging from 15 to 150 kDa. Polyclonal antibodies against pORF2 were generated and specifically recognized the purified protein in immunoassays, with detection observed at dilutions from 1:500 to 1:3000. No cross-reactivity was observed with negative controls, but a non-specific ~75 kDa band was detected in *E. coli* extracts.

**Conclusion.** A protocol for expressing, detecting, and purifying the recombinant 6xHis-pORF2 protein from PMeV-Mx in *E. coli* was established. Rabbit polyclonal antibodies recognized the target protein in bacterial fractions, though further optimization is needed to enhance specificity. These antibodies will support future diagnostic development and protein characterization in plants.

**Keywords:** Papaya meleira, Recombinant proteins, Antibodies, Umbra-like viruses, PMeV-Mx

## INTRODUCTION

Papaya meleira, also known as papaya sticky disease, is typically characterized by a spontaneous exudation of latex from the green fruits (Figure 1). The exuded latex undergoes oxidation, which can cause necrotic spots on fruits, resulting in a sticky appearance. Necrotic lesions have also been observed on the tips of young leaves in Solo group varieties in Brazil (Rodríguez *et al.*, 2009; Perez-Brito *et al.*, 2012). Papaya meleira can lead to severe economic losses for papaya growers (Ventura *et al.*, 2004; Perez-Brito *et al.*, 2012). It was first reported in Brazil (Nakagawa *et al.*, 1987) at the end of the decade of the 80's and now it has extended to several countries in Latin America, including Mexico, Ecuador, Colombia and Costa Rica (Perez-Brito *et al.*, 2012; Quito-Avila *et al.*, 2023) as well as to Australia (Pathania *et al.*, 2019). It is caused by virus complexes, a double stranded RNA genome virus tentatively assigned to the *Fusagraviridae* family and a positive sense single stranded RNA [(+) ssRNA ssRNA] genome, an umbra-like virus, proposed into the *Tombusviridae* family (Sa Antunes *et al.*, 2016; Maurastoni *et al.*, 2023; Quito-Avila *et al.*, 2023). Papaya umbra-like viruses associated to meleira disease are Papaya meleira virus 2 (PMeV2) in Brazil, Papaya virus Q (PpVQ) in Ecuador and Papaya meleira virus Mexican variant (PMeV-Mx) in Mexico (Quito-Avila *et al.*, 2015; Zamudio-Moreno *et al.*, 2015; Sa Antunes *et al.*, 2016). Based on umbraviruses demarcation criteria (Taliany *et al.*, 2003) papaya umbra-like viruses are considered separated species (Cornejo-Franco *et al.*, 2021).

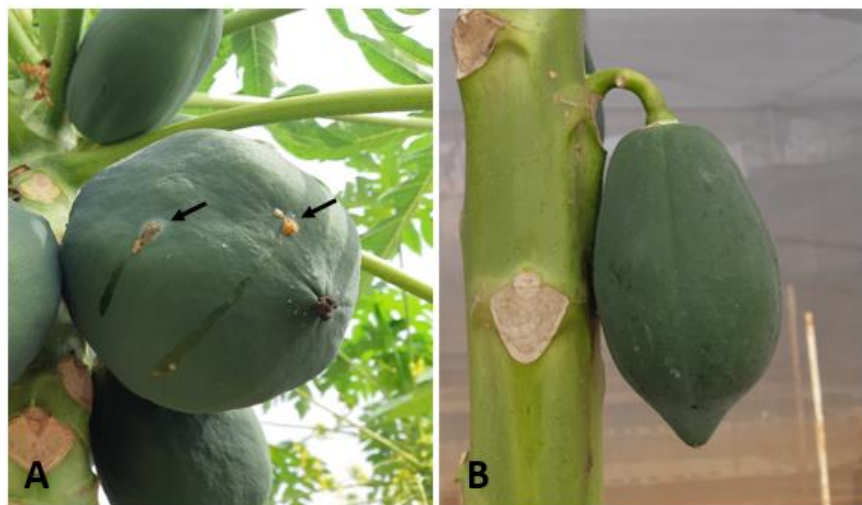


**Figure. 1.** Fruits of *Carica papaya* cv. Maradol plants grown in the screen house. A) Papaya fruits infected with PMeV-Mx showing the typical meleira disease symptom of spontaneous latex exudation. B) Fruit of mock-inoculated papayas (Healthy).

Because the genomes of umbra-like viruses (ULVs) do not encode a capsid protein, they have been considered as sub viral entities, and also referred as umbra-like associated RNAs (ulaRNAs) (Liu *et al.*, 2021). There are three classes of plant ULVs, with genomes varying in size from 3500 to 4500 nt, with two to five open reading frames (ORFs) (Cornejo-Franco *et al.*, 2021; Liu *et al.*, 2021; Redila *et al.*, 2021; Tahir *et al.*, 2021).

Papaya ULVs belong to class 1, with genomes of 4376 to 4515 nt that contain two ORFs, followed by a large non-coding RNA. ORF1 encodes a putative protein of 31 to 38 kDa, of unknown function. ORF2 encodes a protein of 45-54 kDa that contains the eight motifs of RNA dependent RNA Polymerases (RdRp) in (+) ssRNA viruses, phylogenetically related to the RdRp of umbraviruses (Zamudio-Moreno *et al.*, 2015; Sa Antunes *et al.*, 2016; Cornejo-Franco *et al.*, 2021; Liu *et al.*, 2021). Two motifs associated with -1 ribosomal frameshifting (-1 FS) have been identified in the genome of ULVs, between ORF1 and ORF2. A slippery region with the consensus sequence X XXY YYZ (the heptanucleotide) and a downstream RNA secondary structure in the form of a hairpin or pseudoknot. This suggests the possibility that the RdRp is expressed through a -1 FS mechanism in ULVs as the product of ORF1 and ORF2 (Liu *et al.*, 2021; Cornejo-Franco *et al.*, 2021). Ribosomal frameshifting contributes to the control of the stoichiometry of the proteins under its regulation, which is crucial for successful viral infection (Penn *et al.*; 2020). It is common in members of the *Tombusviridae* family, and its occurrence has been experimentally demonstrated in the umbravirus *Pea enation mosaic virus 2* (PEMV2) (Gao and Simon, 2016) and in class 2 ULV *Citrus yellow vein associated virus* (CYVaV), where an 81 kDa protein, product of ORF1 and ORF2, has been observed using *in vitro* transcription/translation assays (Liu *et al.*; 2021). However, the -1FS mechanism remains to be demonstrated for papaya ULVs.

To date, viral proteins exhibiting meleira disease have not been detected in plants (Rodrigues *et al.*, 2009), and no antibodies for diagnosis have been produced. The development of antibodies specific to viral regions such as the RdRp provides a valuable toolkit for studying and monitoring plant diseases. They are also valuable in epidemiology, allowing the tracking of the spread and evolution of viral pathogens in plant populations, information crucial for developing more efficient management strategies and predicting future outbreaks (Rubio *et al.*, 2020; Buja *et al.*, 2021). Furthermore, antibodies enable functional studies of viral proteins, such as polymerases, including their expression and interaction with host factors, knowledge essential to develop antiviral strategies and understanding the molecular basis of viral replication (Bolanos-Garcia and Davies, 2006; Trier *et al.*, 2019; Rubio *et al.*, 2020). However, it has proven difficult to purify RdRps directly from host cells due to their low expression levels (Cevik *et al.*, 2008). Also, they are usually associated with membrane structures which difficult the isolation due to stability problems (Laliberte and Sanfaçon, 2010; Hull, 2014). These problems can be overcome by expressing recombinant proteins in *E. coli* (Cevik *et al.*, 2008). Previous studies have demonstrated the viability of this strategy for the development of antibodies against the RdRp of the *Citrus tristeza virus* (CTV), which led to the detection and localization of the protein in citrus tissue infected with CTV (Cevik, 2001; Cevik *et al.*, 2008). Likewise, the polymerases of the *Tobacco vein mottling virus* (TVMV), *Bamboo mosaic virus* (BaMV) and SARS-CoV-2 have been expressed in *E. coli*, obtaining antibodies, and with them, advances in the characterization of their functions and catalytic activity (Hong and Hunt, 1996; Li *et al.*, 1998; Dangerfield *et al.*, 2021; Madru *et al.*, 2021).

This study aimed to develop a method for producing and purifying recombinant PMeV-Mx ORF2 encoded protein in *E. coli* and generate specific antibodies for its detection, a key step to further virus diagnostic and basic research.

## MATERIALS AND METHODS

**Papaya plants as virus reservoir.** Papaya seeds Maradol variety, were germinated and seedlings were transferred to an anti-aphids screened green house with soil bedding. Three-month-old seedlings were inoculated with the latex of fruits obtained from plants symptomatic for papaya meleira disease and the presence of PMeV-Mx was confirmed on six of these plants by RT-PCR as was previously reported (Zamudio-Moreno *et al.*, 2015).

**Sequence analysis.** The partial sequence of the PMeV-Mx genome, which includes the complete coding region (NCBI GenBank nucleotide database accession number KF214786) was analyzed using UGENE software. ORFs were identified, as well as the putative slippery site (heptameric sequence) as described previously (Cornejo-Franco *et al.*, 2021). The putative translated products were predicted, either individually or by -1 FS spanning ORF1 and ORF2.

**Construction of plasmids.** The PMeV-Mx ORF1 and ORF2 were amplified by PCR with primers CB157/CB158 and CB183/CB184 respectively (Table 1), using 2 µL of the first strand cDNA obtained with RNA from latex of fruits of infected papaya plants as template as previously reported (Zamudio-Moreno *et al.*, 2015). The PCR reaction was carried out in a 25 µL volume [PCR buffer (1x), 1.5 mM MgCl<sub>2</sub>, 0.2 mM dNTPs, 0.2 µM of primers, 2 U of Platinum™ Taq DNA Polymerase (Invitrogen, Massachusetts, USA)]. The PCR product was purified with QIAquick PCR Purification Kit (Qiagen, Hilden, Germany) and ligated into pGEM-T Easy following the suppliers' instructions (Promega, Wisconsin, USA) to produce pCB251 (pGEM-T Easy:ORF1) and pCB233 (pGEM-T Easy:ORF2). The insert was confirmed by PCR, with primers that target the promoters SP6 and T7 regions of pGEM-T Easy (Table 1). Plasmid DNA was purified with QIAprep Spin Miniprep Kit (Qiagen, Hilden, Germany) and sequenced (Macrogen Inc., Seoul, Korea).

**Table 1.** Primers used to clone PMeV-Mx ORF1 and ORF2 in pDEST17 vector, to generate plasmids pCB252 and pCB253, respectively.

Primer	Sequence (5' to 3') <sup>y</sup>	Binding region <sup>z</sup>
CB135	TAATACGACTCACTATAGGG	Promotor T7 of pGEM-T Easy
CB136	ATTTAGGTGACACTATAGAA	Promotor SP6 of pGEM-T Easy
CB157	<b>ATGAACATTT</b> CGAACATTCCC	ORF1 sense orientation
CB158	GGATCCTTACGGGCAACAGAAAA	ORF1 anti-sense orientation
CB183	aattagatc <b>ATG</b> GTTTATACCTTCATCAAA	ORF2 sense orientation
CB184	taattaagctt <b>CTA</b> AGGGGTTAAGATAAGC	ORF2 anti-sense orientation
CB107	aaaaagcaggcttc <b>ATGAACATTT</b> CGAACATTCCCGT	ORF1 sense orientation and <i>attB1</i> site
CB108	agaaagctgggtc <b>TTACGGGCAACAGAAA</b> AGGACGA	ORF1 anti-sense orientation and <i>attB2</i> site
CB191	aaaaagcaggctcc <b>ATG</b> GTTTATACCTTCATCAAA	ORF2 sense orientation and <i>attB1</i> site
CB193	agaaagctgggtc <b>AGGGGTTAAGATA</b> ACCCTAGG	ORF2 anti-sense orientation and <i>attB2</i> site
CB194	ggggacaagttgtacaaaaagcaggct	<i>attB1</i> adapter
CB195	ggggaccactttgtacaagaagctgggt	<i>attB2</i> adapter

<sup>y</sup>Lowercase letters indicate non-viral sequences, such as restriction sites and extra nucleotides (CB183 and CB184), or recombination sites (CB107, CB108, CB191, CB193, CB194 and CB195). Bold font signals stop and start codons.

<sup>z</sup>ORF, open reading frame; *attB*, site specific attachment for Gateway recombination.

The amplicons containing PMeV-Mx ORF1 and PMeV-Mx ORF2 were transferred into the Gateway plasmid pDONR221 (Invitrogen Massachusetts, USA) to generate pCB247 (pDONR221:ORF1) and pCB249 (pDONR221:ORF2), respectively. Later on, they were recombined into pDEST17 (Invitrogen, Massachusetts, USA) to generate pCB252 (pDEST17:ORF1) and pCB253 (pDEST17:ORF2), respectively. Primers for PMeV-Mx ORF1 and ORF2 adding half of the *attB* sites (CB107/CB108 and CB191/CB193, respectively), were used, as well as a second pair of adapter primers to complete the *attB* sites (CB194/CB195) (Table 1). The reaction mixture and PCRs were performed following the Gateway Technology manual (2021) (Invitrogen, Massachusetts, USA). The final PCR products were recombined respectively with the entry vector pDONR221 (Invitrogen, Massachusetts, USA), using the BP CLONASE enzyme mixture (Invitrogen, Massachusetts, USA), following the manufacturer's instructions. The recombination products were introduced into *E. coli* DH5 $\alpha$  competent cells and selected on Luria Broth (LB) agar plates supplemented with 100  $\mu\text{g mL}^{-1}$  kanamycin. The resulting entry vectors, pCB247 and pCB249, were sequenced (Macrogen Inc., Seoul, Korea). Plasmid DNA was extracted and used for recombination with the destination vector pDEST17 (Invitrogen, Massachusetts, USA) to generate pCB252 and pCB253, respectively using the LR CLONASE enzyme mixture (Invitrogen, Massachusetts, USA), following the manufacturer's instructions. The products were introduced into *E. coli* DH5 $\alpha$  cells, selected on agar LB plates supplemented with 100  $\mu\text{g mL}^{-1}$  ampicillin. Plasmid DNA was sequenced and used to transform the *E. coli* BL21 strain.

**Expression and purification of recombinant proteins in *E. coli*.** A time course expression was first conducted. *E. coli* BL21 cells carrying pCB253 were used to inoculate 5 mL LB medium with 100  $\mu\text{g mL}^{-1}$  ampicillin, and incubated shaking at 200 rpm, during 14 h at 37 °C. From this pre-inoculum, 500  $\mu\text{L}$  were transferred to 300 mL medium under the same conditions, until reaching an optical density of 0.6 at 600 nm wavelength. 40 mL of medium were removed and stored as uninduced control. 1 mM isopropyl  $\beta$ -D-thiogalactopyranoside (IPTG) was added to the remaining inoculum and incubated for 6 h at 37 °C shaking at 200 rpm. Every hour, 40 mL of medium were removed. The induced and non-induced bacterial cultures were centrifuged at 5000 rpm for 10 minutes, the pellet was re-suspended in 2 mL protein extraction buffer for denaturing conditions (100 mM  $\text{NaH}_2\text{PO}_4$ , 10 mM Tris-Cl; 8 M Urea, pH 8.0) as described in The QIAexpressionist Manual, 2003 (Qiagen, 2003). The suspension was sonicated on ice with 20-second cycles, until viscosity was lost; treated with 0.2 mM phenylmethylsulfonyl fluoride (PMSF) and centrifuged at 12,000 rpm and 4 °C during 10 min. The supernatant was stored at -80 °C, and the pellet resuspended in 3 mL protein extraction buffer.

For immunodetection of recombinant proteins, *E. coli* protein extracts were first incubated for 3 h at 92 °C, separated on a 12 % sodium dodecyl sulfate (SDS) polyacrylamide gel and transferred to a polyvinylidene fluoride (PVDF) membrane, applying 100 volts for 1 h. Membranes were blocked by incubation with 0.1 % PBS-T/5 % milk (w/v) for 1 h at room temperature followed of three 20 min washes with 0.1 % PBS-T, and the subsequent incubation with a 1:1000 dilution of the anti-His tag monoclonal antibody coupled to horseradish peroxidase (HRP) (Invitrogen #R93125,

Massachusetts, USA) during 12 h at 4 °C. Followed by two washes with 0.1 % PBS-T. After substrate incubation (ECL, Thermo Fisher Scientific, Pierce, Massachusetts, USA), images were registered on a Gel Doc XR+ documentation system (Bio-Rad Laboratories, Inc., California, USA). For this assay, the 6xHis-GST-8xHis recombinant protein, expressed from pET42b (Novagen, Merck KGaA, Darmstadt, Germany) was used as positive control.

To purify recombinant proteins, *E. coli* BL21 cells were grown in a 500 mL culture 2 h after induction, as described above, except for the amount of extraction buffer (6 mL) and following instructions in the QIAexpressionist Manual, 2003 (Qiagen, 2003). The recombinant proteins were affinity purified in a column packed with nickel-nitrilotriacetic acid (Ni-NTA) resin (Qiagen) and washed three times with buffer pH 6.3. Two elutions were obtained, decreasing the pH from 5.9 to 4.5.

**Production of Antisera.** Purified recombinant proteins were separated on 12 % SDS-polyacrylamide gels. The band corresponding to the recombinant 6xHis-pORF2 protein was cut from the gel and lyophilized. The protein was then mixed with 200 µL PBS, quantified in a NanoDrop 2000 Spectrophotometer (Thermo Fisher Scientific, Massachusetts, USA), and then mixed with 200 µL of complete adjuvant for the first inoculation and incomplete adjuvant for the following ones (Amero *et al.*, 1988). Subsequently, the emulsions were subcutaneously inoculated at one or two points on the back of two rabbits. Before immunization, 500 µL of rabbit blood was extracted to verify the absence of reactivity to the antigen in the pre-immune serum. The first immunization (100 µg of protein) was performed and repeated two weeks later (500 µg of protein), followed by a first collection of 3 mL of blood ten days later. Subsequently, the rabbits rested for four weeks, and a final immunization (100 µg of protein) was performed, followed by a collection of 5 mL of blood seven days later with a neonatal catheter. The blood was centrifuged at 3000 rpm, during 20 min at 4 °C and the antisera were stored at -20 °C (Amero *et al.*, 1988; Pihl *et al.*, 2015).

To verify the serum reactivity and to identify the optimal working dilution a dot blot was performed. The following dilutions were evaluated: 1:500, 1:1000, 1:2000, 1:3000, and 1:4000. The assay was conducted as follows: 10 µL of antisera was added to a nitrocellulose membrane (1 cm<sup>2</sup>), which was then blocked with a solution of 5 % non-fat powdered milk in 1X PBS-T for 1 h, with agitation at room temperature. Afterward, the membrane was incubated overnight at 4 °C with different dilutions of the primary antibody. Three washes with PBS-T were then performed, followed by incubation with the secondary anti-rabbit antibody conjugated with HRP (dilution 1:3000) (Promega #W4011, Wisconsin, USA) for 2 h at room temperature, and developed as described above.

To confirm the specificity of the antisera and the antibodies, immunodetection assays were performed. In this case, detection was carried out in nitrocellulose membranes with a 1:1000 dilution of anti-pORF2 as the primary antibody, followed of incubation with a 1:3000 dilution of anti-rabbit secondary antibody coupled to HRP (Promega #W4011, Wisconsin, USA). For this assay two recombinant proteins fused to His tags were used as negative controls, 6xHis-GST-8xHis expressed from the pET42b plasmid (Novagen, Merck KGaA, Darmstadt, Germany) and 6xHis-pORF1 expressed from pCB252.

## RESULTS

**The predicted putative proteins from PMeV-Mx.** PMeV-Mx genome contains two ORFs, from positions 1 to 963 (ORF1) and 1231 to 2437 (ORF2) encoding two putative proteins of 35 and 45.6 kDa, respectively, named here pORF1 and pORF2. It also contains a slippery site at position 942 to 948 (UCCUUUU), a putative signal for -1 FS, which could generate a putative protein of 91.3 kDa, as a product of ORF1 and ORF2 (Figure 2), as proposed previously for BabVQ (Cornejo-Franco *et al.*, 2021). However, sequence analysis of the PMeV-Mx genome and proteins in this study does not support this premise, because stop codons are introduced in the intergenic region, and thus creating a potential truncated protein.

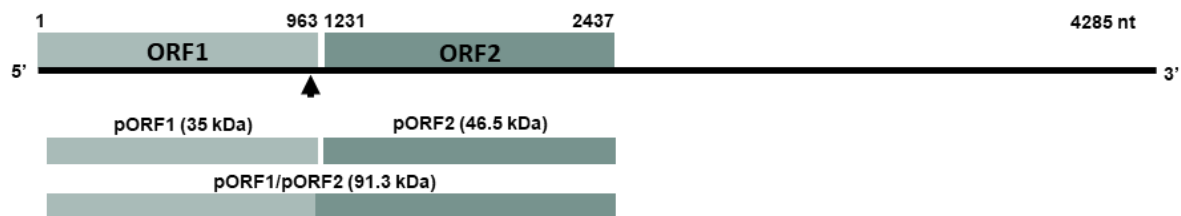


**Figure 2.** Genomic organization of PMeV-Mx. Numbers indicate the nucleotide (nt) positions and the total number of nt in the genome. Solid boxes in the genome represent ORF1 and ORF2, respectively. Solid boxes below indicate the putative proteins, product of ORF1 and ORF2 (pORF1 and pORF2, respectively) and the putative fusion product of -1 ribosomal frameshifting (pORF1/pORF2). The arrow indicates the position of the heptanucleotide.

**Expression and purification of a recombinant 6xHis-pORF2 fusion protein.** In order to determine the best conditions for expression of the protein product of PMeV-Mx ORF2 (pORF2) fused to the 6xHis tag (6xHis-pORF2), a time course was done. A protein migrating between the 37 and 50 kDa markers was observed 1 h after induction with IPTG but not in the non-induced treatment (Figure 3). These results are consistent with the estimated molecular mass of ~46.5 kDa for the recombinant protein 6xHis-pORF2. A notable increase in expression is observed from 2 h to 6 h post-induction (Figure 3).

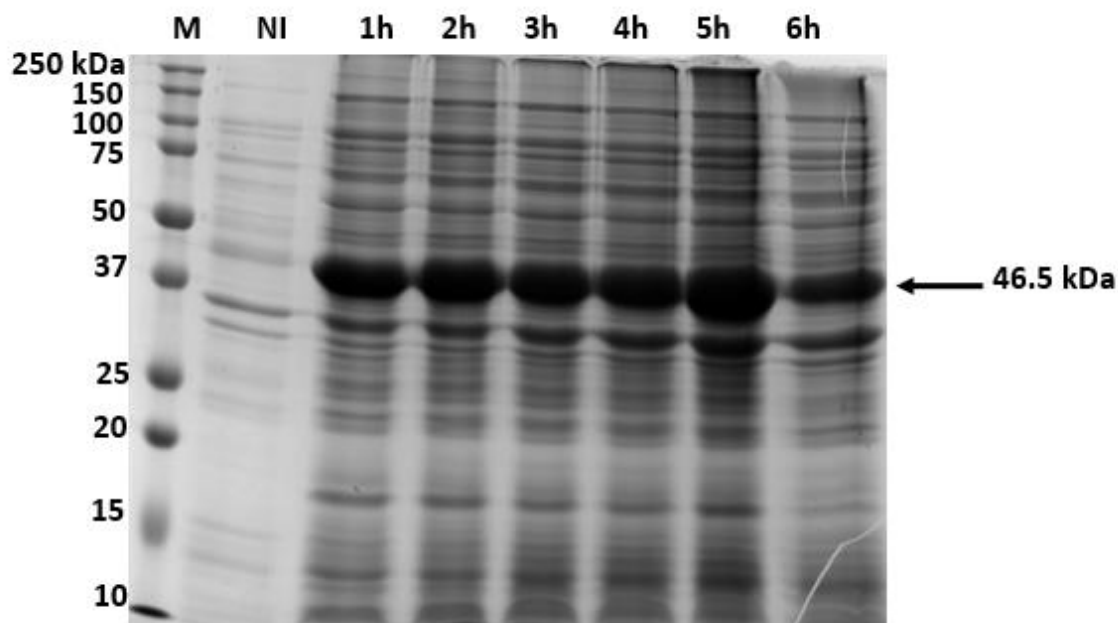


**Figure 3.** Time course of PMeV-Mx 6xHis-pORF2 expression using insoluble crude *E. coli* lysate to establish the optimal induction period for expression. Expression of 6xHis-pORF2 was induced with 1 mM IPTG, at 37 °C. Aliquots were removed at the times indicated (1 to 6 h after IPTG induction) and proteins were visualized by Coomassie-stained SDS gel. M, Bio-Rad 10-250 kDa marker; NI, non-induced control. The arrow indicates the 46.5 kDa 6xHis-pORF2 protein.

Considering the data from the time course assay, a 2 h induction period was selected to maximize protein yield. The 6xHis-pORF2 PMeV-Mx recombinant protein was detected by western blot with anti-His antibodies. As expected, ~46.5 and ~28 kDa proteins were observed (Figure 4 B, lanes 3 and 4) corresponding to the 6xHis-pORF2 and 6xHis-GST-8xHis recombinant proteins, respectively. This result confirmed that the recombinant PMeV-Mx pORF2 protein contained the His-tag and its overall integrity (Figure 4). The purification of the recombinant protein with Ni-NTA resin is shown in Figure 5. An intense band of the expected size, ~46.5 kDa, was observed in each elution. Likewise, less intense bands of larger and smaller masses, ranging from 15 to 150 kDa were also observed in both the elution, and the resin. Following the previously stated conditions eight purifications from 20 mL of cellular fractions were carried out. As a result, 800 µg of the purified 6xHis-pORF2 were obtained for downstream applications, such as antibody production.

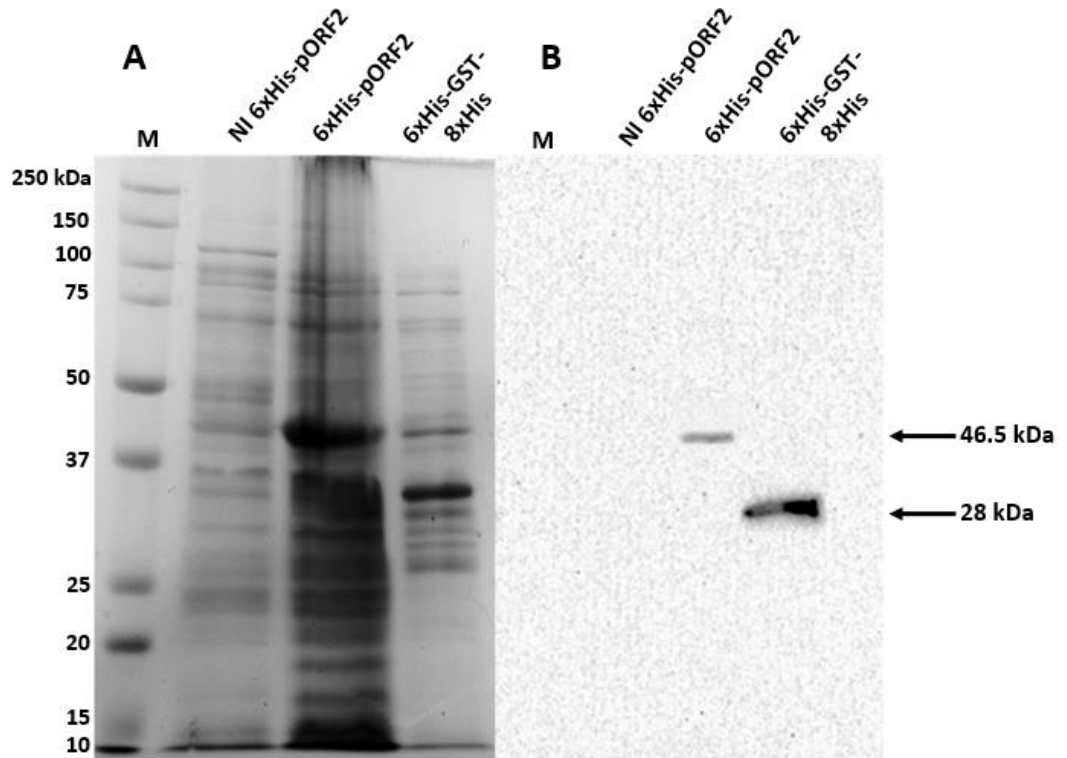


**Figure 4.** Detection of PMeV-Mx 6xHis-pORF2 in *E. coli* crude lysates by monoclonal anti-His antibodies. A) Coomassie-stained SDS gel. B) Western blot in PVDF membranes incubated with a 1:1000 dilution of the anti-His tag monoclonal antibody coupled to horseradish peroxidase (HRP). M, Bio-Rad 10-250 kDa marker; NI and 6xHis-GST-8xHis, non-induced and positive controls, respectively; 6xHis-pORF2, cellular fraction with recombinant PMeV-Mx pORF2 expressed in BL21 cells. The arrows indicate the 46.5 kDa 6xHis-pORF2 and the 28 kDa 6xHis-GST-8xHis proteins, respectively.

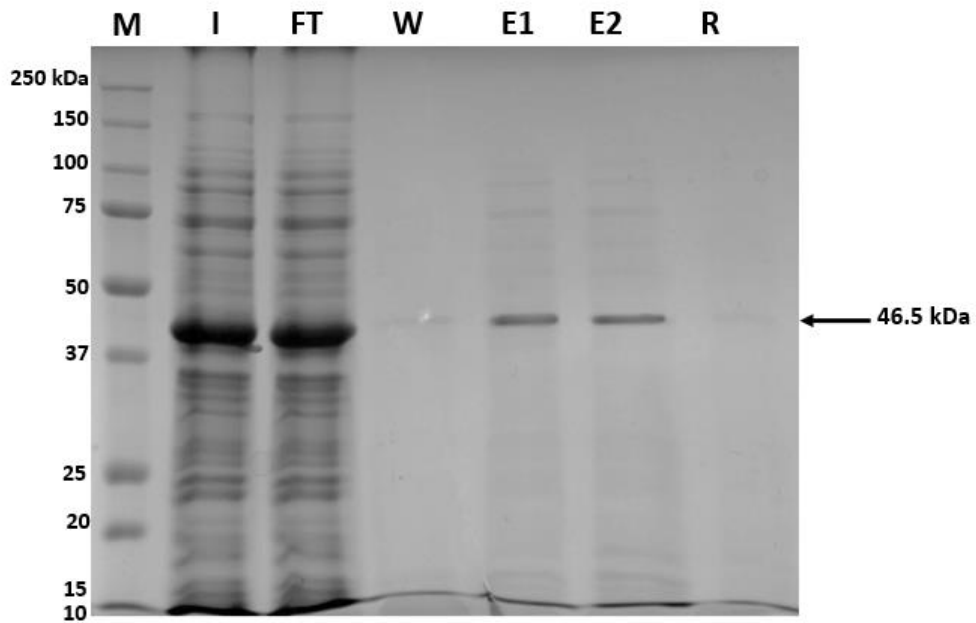


**Figure 5.** Purification of PMeV-Mx 6xHis-pORF2 with Ni-NTA Agarose under denaturing conditions. M, Bio-Rad 10-250 kDa marker; I, input; Ft, flow-through; E1 and E2, first and second eluates, respectively; R, resin. The arrow indicates the 46.5 kDa 6xHis-pORF2 protein.

**Specificity of anti-pORF2 polyclonal antibodies.** Pre-immune serum was obtained to confirm the absence of reactivity against PMeV-Mx 6xHis-pORF2. Furthermore, the serum titer was determined after immunization, and a signal was detected with dilutions 1:500 to 1:3000. Dilution 1:1000 was used to continue the analysis. The specificity of the anti-pORF2 antibodies was evaluated using immunoassays (Figure 6). A signal of ~46.5 kDa was detected on the cellular fractions corresponding to 6xHis-pORF2. This confirmed the presence of the target protein in the protein extracts and demonstrated the ability of the antibodies to specifically recognize it. The absence of a signal at the expected sizes on the negative controls, ~28 kDa band for 6xHis-GST-8xHis and ~35 kDa for PMeV-Mx 6xHis-pORF1 further confirmed the specificity. These negative controls were included to ensure that the observed signal was not due to non-specific interactions with other proteins present in the cellular fractions or the His tag. Nonetheless, the antibody was also found to be non-specific for *E. coli* proteins, since a protein of approximately 75 kDa was detected in the lanes corresponding to the non-induced cellular fraction and induced fractions for 6xHis-pORF1, 6xHis-GST-8xHis and 6xHis-pORF2 (Figure 6, B).

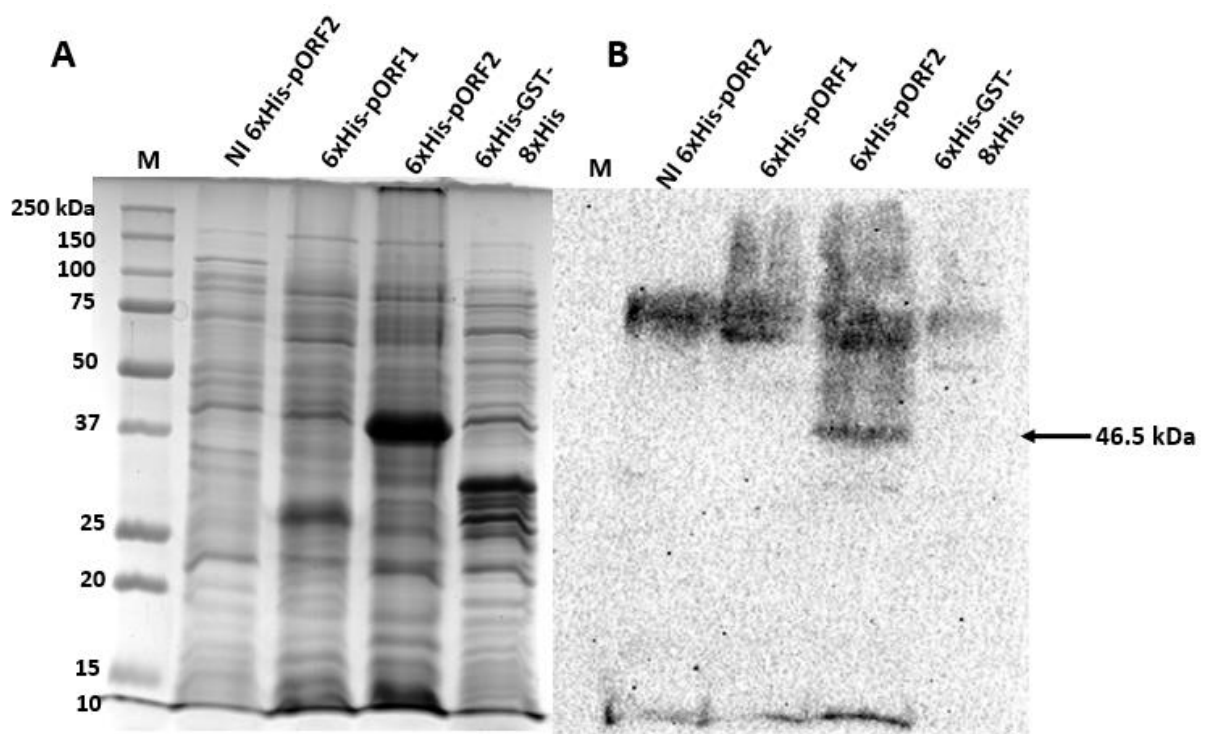


**Figure 6.** Detection of PMeV-Mx 6xHis-pORF2 in *E. coli* crude lysate with anti-pORF2 antibodies. A) Coomassie-stained SDS gel. B) Western blot (Nitrocellulose membrane) incubated with the anti- PMeV-Mx pORF2 polyclonal antibody (dilution 1:1000), and the anti-rabbit coupled to horseradish peroxidase (HRP) secondary antibody (dilution 1:3000). M, Bio-Rad 10-250 kDa marker; NI, non-induced cellular fraction. 6xHis-pORF1 and 6xHis-GST-8xHis were used as negative controls. The arrow indicates the 46.5 kDa 6xHis-ORF2 protein.

## DISCUSSION

The present manuscript describes for the first time the expression in *E. coli* of the recombinant protein encoded by the ORF2 of PMeV-Mx, its purification as well as the development of rabbit polyclonal antibodies. The successful expression of the recombinant protein in *E. coli* represents a valuable tool for both phytopathological and protein characterization studies, as it presents several advantages. *E. coli* is a well-established expression system for recombinant proteins, known for its high yields and simplified purification procedures (Jia and Jeon, 2016). This approach facilitates the production of large quantities of recombinant protein for detailed biochemical and biophysical characterization. Obtaining such quantities directly from plant tissues can be challenging due to low RdRp expression levels and the presence of contaminating proteins. Furthermore, expressing a viral protein in *E. coli* offers several advantages over cell-free *in vitro* expression systems, including lower costs, simpler procedures, and the ability to perform post-translational modifications and protein assembly (Rosano and Ceccarelli, 2014; Jia and Jeon, 2016).

In this study, the 46.5 kDa recombinant protein expressed by the ORF2 of PMeV-Mx (6xHis-pORF2) was observed at 1 h post induction and throughout a 6 h time course in *E. coli* insoluble crude lysates. This was expected since viral RNA polymerases are usually associated to membranes (Laliberte and Sanfaçon, 2010; Hull, 2014). Although the highest expression was observed at 5 h post induction (Figure 3), a 2 h time point was selected for purification in order to decrease the formation of inclusion bodies, which usually takes place when expressing membrane associated proteins at high levels (Qiagen, 2003). Western blot results with anti-His antibodies (Figure 4) corroborated that the 46.5 kDa protein contained the 6xHis tag and corresponded to the recombinant protein. This protein was successfully purified (Figure 5) and used to raise rabbit polyclonal antibodies.

Anti-pORF2 antibodies were able to detect the recombinant PMeV-Mx 6xHis-pORF2 in *E. coli* cell extracts, and did not detect either the recombinant PMeV-Mx 6xHis-pORF1 or the 8xHis-GST-6x proteins in western blots, demonstrating their specificity (Figure 6). Anti-pORF2 antibodies also detected a ~75 kDa protein in all *E. coli* extracts (Figure 6). These could be attributed to non-specific bacterial protein binding to the Ni-NTA resin during protein purification, as shown by Ryan and Henehan, 2013. Optimizing Ni-NTA resin conditions (salt concentration, pH, and imidazole concentration) can reduce non-specific binding. Additionally, testing different Ni-NTA resins for better binding capacity and selectivity is recommended (Wang *et al.*, 2020). Furthermore, including a size-exclusion or ion exchange chromatography step (Saraswat *et al.*, 2013) and optimizing elution conditions (pH or imidazole concentration) would ensure pure elution of the target protein (Soltaninasab *et al.*, 2022). In addition, antibodies purification by affinity chromatography could also improve their specificity and sensibility for plant diagnosis (Saraswat *et al.*, 2013).

Antibodies are also necessary for fundamental studies. The protein encoded by ORF2 in PMeV-Mx and other class 1 papaya ULVs, contain the eight motifs present in RNA-dependent RNA polymerases. However, their expression mechanisms and function in plants have not been characterized. Replication of members of the genus *Tombusvirus*, in the *Tombusviridae* family, has been extensively studied. The RdRp of Tomato bushy stunt virus (TBSV) is a 92 kDa protein produced by stop codon readthrough of ORF1 spanning ORF2. While its replicase is formed by the interaction of the replication auxiliary protein

p33, encoded by ORF1, and p92 (Salonen *et al.*, 2005; den Boon *et al.*, 2010). It has been proposed that a RdRp of ~90 kDa could be produced as a result of -1 RF mechanism for class 1 papaya ULVs (Quito-Avila, *et al.*, 2023), as has been shown *in vitro* for class 2 ULVs and umbraviruses (Liu *et al.*, 2021). However, this has not been demonstrated and needs to be addressed. Antibodies could be used to detect viral proteins in plants and further study their RdRp expression and function.

## CONCLUSIONS

In this study, we successfully established a protocol for the expression, detection, and purification of the recombinant 6xHis-pORF2 protein of PMeV-Mx in *E. coli*, the putative RdRp. Anti-pORF2 antibodies detected the target protein in *E. coli*, although further optimization is still necessary, to increase their specificity in *E. coli* cell extracts.

## LIMITATIONS

In this study we successfully expressed and purified the recombinant PMeV-Mx ORF2 protein in *E. coli* and generated specific antibodies, providing a valuable tool for viral protein characterization and future diagnostic applications. However, although the approach used has proven to be effective, further adjustments could enhance its scope and applicability. The expression system may not fully replicate the native folding and post-translational modifications occurring in plant cells. The presence of non-specific bands in western blot assays highlights the need for further optimization of Ni-NTA purification conditions to improve protein purity. Furthermore, while the generated antibodies successfully detected the recombinant protein in *E. coli* extracts, their performance in plant tissues remains to be assessed. Future studies are necessary to investigate the expression and function of the PMeV-Mx RdRp in infected plants, which could provide insights into its role in viral replication.

## Conflicts interest

The authors declare that they have no conflict of interest.

## Funding

This project was financed by CONAHCYT, grant AS-1-19850 to LLO. CONAHCYT also provided scholarships to WS, JAAQ and AFT.

## ACKNOWLEDGMENTS

We thank to M.C. Roberto Ku-Cauich, Dr. Ligia Brito-Argaez, and M.C. Miguel Ztzec-Simá for technical help.

### Author contributions

Conception, LLO; experimental design, WS, EC, IIF, LLO; experimental execution, WS, JAAQ, MCP, AFT, LLO; experiment verification, JAAQ, MCP, LLO; data analysis/interpretation, WSH, EC, LLO; manuscript preparation, WS, LLO; manuscript editing and review, WS, JAAQ, MCP, AFT, EC, IIF, LLO. All authors have read and agreed to the published version of the manuscript.

### REFERENCES

- Amero SA, James TC and Elgin SC. 1988. Production of antibodies using proteins in gel bands. *Methods in Molecular Biology* (Clifton, N.J.) 3: 355-362. <https://dx.doi.org/10.1385/0-89603-126-8:355>
- Arur S and Schedl T. 2014. Generation and purification of highly specific antibodies for detecting post-translationally modified proteins in vivo. *Nature Protocols* 9: 375-395. <https://dx.doi.org/10.1038/nprot.2014.017>
- Bolanos-Garcia VM and Davies OR. 2006. Structural analysis and classification of native proteins from *E. coli* commonly co-purified by immobilised metal affinity chromatography. *Biochimica et Biophysica Acta* 1760: 1304-1313. <https://dx.doi.org/10.1016/j.bbagen.2006.03.027>
- Buja I, Sabella E, Monteduro AG, Chiriaco MS, De Bellis L, Luvisi A and Maruccio G. 2021. Advances in plant disease detection and monitoring: From traditional assays to in-field diagnostics. *Sensors (Basel, Switzerland)* 21. <https://dx.doi.org/10.3390/s21062129>
- Cevik B. 2001. Characterization of the RNA-dependent RNA polymerase gene of Citrus tristeza Closterovirus. (PhD), Florida University, USA. Retrieved from <http://ufdcimages.uflib.ufl.edu/UF/00/10/07/35/00001/DissertationBC.PDF>
- Cevik B, Lee RF and Niblett CL. 2008. *In vivo* and *in vitro* expression analysis of the RNA-dependent RNA polymerase of Citrus tristeza virus. *Archives of Virology* 153: 315-321. <https://dx.doi.org/10.1007/s00705-007-1060-8>
- Cornejo-Franco JF, Flores F, Mollov D and Quito-Avila DF. 2021. An umbra-related virus found in babaco (*Vasconcellea × heilbornii*). *Archives of Virology* 166: 2321-2324. <https://dx.doi.org/10.1007/s00705-021-05117-8>
- Dangerfield TL, Huang NZ and Johnson KA. 2021. Expression and purification of tag-free SARS-CoV-2 RNA-dependent RNA polymerase in *Escherichia coli*. *STAR Protocols* 2: 100357. <https://dx.doi.org/10.1016/j.xpro.2021.100357>
- den Boon JA, Ahlquist P. 2010. Organelle-like membrane compartmentalization of positive-strand RNA virus replication factories. *Annual Review of Microbiology*, 64: 241-256, <https://dx.doi.org/10.1146/annurev.micro.112408.134012>
- Gao F and Simon AE. 2016. Multiple Cis-acting elements modulate programmed -1 ribosomal frameshifting in Pea enation mosaic virus. *Nucleic Acids Research* 44: 878-895. <https://dx.doi.org/10.1093/nar/gkv1241>
- Hong Y and Hunt AG. 1996. RNA polymerase activity catalyzed by a potyvirus-encoded RNA-dependent RNA polymerase. *Virology* 226: 146-151. <https://dx.doi.org/10.1006/viro.1996.0639>
- Hull R. 2014. Chapter 7 - Replication of Plant Viruses. In Hull R (Ed.), *Plant Virology (Fifth Edition)* (pp. 341-421). Boston: Academic Press. <https://dx.doi.org/10.1016/B978-0-12-384871-0.00007-8>

- Jia B and Jeon CO. 2016. High-throughput recombinant protein expression in *Escherichia coli*: current status and future perspectives. *Open Biology* 6. <https://dx.doi.org/10.1098/rsob.160196>
- Laliberté JF and Sanfaçon H. 2010. Cellular remodeling during plant virus infection. *Annual Review of Phytopathology* 48: 69-91. <https://dx.doi.org/10.1146/annurev-phyto-073009-114239>
- Li YI, Cheng YM, Huang YL, Tsai CH, Hsu YH and Meng M. 1998. Identification and characterization of the *Escherichia coli*-expressed RNA-dependent RNA polymerase of bamboo mosaic virus. *Journal of Virology* 72: 10093-10099. <https://dx.doi.org/10.1128/jvi.72.12.10093-10099.1998>
- Liu J, Carino E, Bera S, Gao F, May JP and Simon AE. 2021. Structural analysis and whole genome mapping of a new type of plant virus subviral RNA: Umbravirus-like associated RNAs. *Viruses* 13. <https://dx.doi.org/10.3390/v13040646>
- Liu J and Simon AE. 2022. Identification of Novel 5' and 3' Translation Enhancers in Umbravirus-Like Coat Protein-Deficient RNA Replicons. *Journal of Virology* 96: e0173621. <https://dx.doi.org/10.1128/jvi.01736-21>
- Madru C, Tekpinar AD, Rosario S, Czernecki D, Brûlé S, Sauguet L and Delarue M. 2021. Fast and efficient purification of SARS-CoV-2 RNA dependent RNA polymerase complex expressed in *Escherichia coli*. *PLOS One*. 16: e0250610. <https://dx.doi.org/10.1371/journal.pone.0250610>
- Maurastoni M, TF SA, Abreu EFM, Ribeiro SG, Mehta A, Sanches MM, Fontes W, Kitajima EW, Cruz FT, Santos AMC, Ventura JA, Gomes A, Zerbini FM, Sosa-Acosta P, Nogueira FCS, Rodrigues SP, Aragão FJL, Whitfield AE and Fernandes PMB. 2023. A capsid protein fragment of a Fusagra-like virus found in *Carica papaya* latex interacts with the 50s ribosomal protein L17. *Viruses* 15. <https://dx.doi.org/10.3390/v15020541>
- Pathania N, Justo V, Magdalita P, de la Cueva F, Herradura L, Waje A, Lobres A, Cueto A, Dillon N, Vawdrey L, Hucks L, Chambers D, Sun G., Cheesman J. 2019. Integrated disease management strategies for the productive, profitable and sustainable production of high quality papaya fruit in the southern Philippines and Australia (FR2019-89). Australian Centre for International Agricultural Research (ACIAR), Canberra, Australia. [https://www.aciar.gov.au/sites/default/files/project-page-docs/final\\_report\\_hort.2012.113.pdf](https://www.aciar.gov.au/sites/default/files/project-page-docs/final_report_hort.2012.113.pdf)
- Penn WD, Harrington HR, Schleich JP, Mukhopadhyay S. 2020. Regulators of Viral Frameshifting: More Than RNA Influences Translation Events. *Annual Review of Virology*, 7(1): 219-238. <https://dx.doi.org/10.1146/annurev-virology-012120-101548>
- Perez-Brito D, Tapia-Tussell R, Cortes-Velazquez A, Quijano-Ramayo A, Nexticapan-Garcez A and Martín-Mex R. 2012. First report of Papaya meleira virus (PMeV) in Mexico. *African Journal of Biotechnology* 11: 13564-13570. <https://dx.doi.org/10.5897/AJB12.1189>
- Pihl TH, Illigen KE and Houen G. 2015. Polyclonal peptide antisera. In Houen G (Ed.), *Peptide Antibodies: Methods and Protocols* (pp. 103-107). New York, NY: Springer New York. [https://doi.org/10.1007/978-1-4939-2999-3\\_11](https://doi.org/10.1007/978-1-4939-2999-3_11)
- Qiagen I. 2003. The QIAexpressionist. A handbook for high-level expression and purification of 6xHis-tagged protein Qiagen I (Ed.) (pp. 128). <https://www.qiagen.com/us/resources/resourcedetail?id=79ca2f7d-42fe-4d62-8676-4cfa948c9435&lang=en>
- Quito-Avila DF, Alvarez RA, Ibarra MA and Martin RR. 2015. Detection and partial genome sequence of a new umbra-like virus of papaya discovered in Ecuador. *European Journal of Plant Pathology* 143: 199-204. <https://dx.doi.org/10.1007/s10658-015-0675-y>

- Quito-Avila DF, Reyes-Proañó E, Cañada G, Cornejo-Franco JF, Alvarez-Quinto R, Moreira L, Grinstead S, Mollov D and Karasev AV. 2023. Papaya sticky disease caused by virus "couples": A challenge for disease detection and management. *Plant Disease* 107: 1649-1663. <https://dx.doi.org/10.1094/pdis-11-22-2565-fe>
- Redila CD; Prakash V; Nouri S. 2021. Metagenomics Analysis of the Wheat Virome Identifies Novel Plant and Fungal-Associated Viral Sequences. *Viruses* 13. <https://dx.doi.org/10.3390/v13122457>.
- Riguero V, Clifford R, Dawley M, Dickson M, Gastfriend B, Thompson C, Wang SC and O'Connor E. 2020. Immobilized metal affinity chromatography optimization for poly-histidine tagged proteins. *Journal of Chromatography. A* 1629:461505. <https://dx.doi.org/10.1016/j.chroma.2020.461505>
- Rodrigues SP, Ventura JA, Aguilar C, Nakayasu ES, Almeida IC, Fernandes PM and Zingali RB. 2011. Proteomic analysis of papaya (*Carica papaya* L.) displaying typical sticky disease symptoms. *Proteomics* 11: 2592-2602. <https://dx.doi.org/10.1002/pmic.201000757>
- Rodrigues SP, Ventura JA, Aguilar C, Nakayasu ES, Choi H, Sobreira TJ, Nohara LL, Wermelinger LS, Almeida IC, Zingali RB and Fernandes PM. 2012. Label-free quantitative proteomics reveals differentially regulated proteins in the latex of sticky diseased *Carica papaya* L. plants. *Journal of Proteomics* 75: 3191-3198. <https://dx.doi.org/10.1016/j.jprot.2012.03.021>
- Rodrigues SP, Ventura JA, Zingali RB and Fernandes PM. 2009. Evaluation of sample preparation methods for the analysis of papaya leaf proteins through two-dimensional gel electrophoresis. *Phytochemical Analysis* 20: 456-464. <https://dx.doi.org/10.1002/pca.1147>
- Rosano GL and Ceccarelli EA. 2014. Recombinant protein expression in *Escherichia coli*: advances and challenges. *Frontiers in Microbiology* 5: 172. <https://dx.doi.org/10.3389/fmicb.2014.00172>
- Rubio L, Galipienso L and Ferriol I. 2020. Detection of plant viruses and disease management: Relevance of genetic diversity and evolution. *Frontiers in Plant Science* 11: 1092. <https://dx.doi.org/10.3389/fpls.2020.01092>
- Rubino L, Scheets K. 2021. *Tombusviruses (Tombusviridae)*. In *Encyclopedia of Virology (Fourth Edition)*, Bamford, D.H., Zuckerman, M., Eds.; Academic Press: Oxford, pp. 788-796.
- Ryan BJ and Henehan GT. 2013. Overview of approaches to preventing and avoiding proteolysis during expression and purification of proteins. *Current Protocols in Protein Science* 5: Unit5.25. <https://dx.doi.org/10.1002/0471140864.ps0525s71>
- Sá Antunes TF, Amaral RJ, Ventura JA, Godinho MT, Amaral JG, Souza FO, Zerbini PA, Zerbini FM and Fernandes PM. 2016. The dsRNA virus Papaya meleira virus and an ssRNA virus are associated with papaya sticky disease. *PLOS One* 11: e0155240. <https://dx.doi.org/10.1371/journal.pone.0155240>
- Salonen A, Ahola T, Kääriäinen L. 2005. Viral RNA replication in association with cellular membranes. *Current Topics in Microbiology and Immunology*, 285: 139-173. [https://dx.doi.org/10.1007/3-540-26764-6\\_5](https://dx.doi.org/10.1007/3-540-26764-6_5)
- Saraswat M, Musante L, Ravidá A, Shortt B, Byrne B and Holthofer H. 2013. Preparative purification of recombinant proteins: current status and future trends. *BioMed Research International* 3:12709. <https://dx.doi.org/10.1155/2013/312709>
- Soltaninasab S, Ahmadzadeh M, Shahhosseini S and Mohit E. 2022. Evaluating the efficacy of immobilized metal affinity chromatography (IMAC) for host cell protein (HCP) removal from anti-HER2 scFv expressed in *Escherichia coli*. *Protein Expression and Purification* 190: 106004. <https://dx.doi.org/10.1016/j.pep.2021.106004>

- Tahir MN; Bolus S; Grinstead SC; McFarlane SA; Mollov D. 2021. A new virus of the family Tombusviridae infecting sugarcane. *Archives of Virology* 166: 961-965, <https://dx.doi.org/10.1007/s00705-020-04908-9>
- Taliansky ME and Robinson DJ. 2003. Molecular biology of umbraviruses: phantom warriors. *Journal of General Virology* 84: 1951-1960. <https://dx.doi.org/10.1099/vir.0.19219-0>
- Trier N, Hansen P and Houen G. 2019. Peptides, antibodies, peptide antibodies and more. *International Journal of Molecular Sciences* 20. <https://dx.doi.org/10.3390/ijms20246289>
- Ventura JA, Costa H and Tatagiba JdS. 2004. Papaya diseases and integrated control. In Naqvi SAMH (Ed.), *Diseases of Fruits and Vegetables: Volume II: Diagnosis and Management* (pp. 201-268). Dordrecht: Springer Netherlands. <https://api.semanticscholar.org/CorpusID:128132558>
- Wang W, Zhou F, Cheng X, Su Z and Guo H. 2020. High-efficiency Ni<sup>2+</sup>-NTA/PAA magnetic beads with specific separation on His-tagged protein. *IET Nanobiotechnology* 14: 67-72. <https://dx.doi.org/10.1049/iet-nbt.2019.0271>
- Zamudio-Moreno E, Ramirez-Prado JH, Moreno-Valenzuela OA and Lopez-Ochoa LA. 2015. Early diagnosis of a Mexican variant of Papaya meleira virus (PMeV-Mx) by RT-PCR. *Genetics and Molecular Research* 14: 1145-1154. <https://dx.doi.org/10.4238/2015.February.6.18>